Electronic Supplementary Information

Conversion pseudocapacitance-featured cost-effective perovskite fluoride $KCuF_3$ for advanced lithium-ion capacitors and lithium-dual-ion batteries

Yuxi Huang[a], Rui Ding[a,*], Qilei Xu[a], Wei Shi[a], Danfeng Ying[a], Yongfa Huang[a], Tong Yan[a], Caini Tan[a], Xiujuan Sun[a], Enhui Liu[a]

[a]Key Laboratory of Environmentally Friendly Chemistry and Applications of Ministry of Education, College of Chemistry, Xiangtan University, Xiangtan, Hunan 411105, P.R. China

[*]**Corresponding Author**

Emails: drm8122@163.com; drm8122@xtu.edu.cn (Rui Ding)

Table of Contents

Experimental section

Synthesis of materials

The chemicals in the experiment are of analytical level (A.R.) and directedly used without further treatment (**Table S1**). The KCF sample is synthesized via a facile one-pot solvothermal route. Firstly, 2.0 mmol $CuCl_2 \cdot 2H_2O$ and 5.0 mmol $KF \cdot 2H_2O$ are dissolved in 35 mL ethylene glycol (EG), the mixture is magnetically stirred and dispersed thoroughly in an ultrasonic bath at 100 W for 30 minutes. Next, the resulting mixture is transferred to a 50 mL reactor, placed in an oven at 180 °C for 12 h. Finally, washed the yielded precipitates after absolute alcohol centrifugation and obtained sample. (The above-mentioned chemicals, agents and materials are listed in the **Table S1**.)

Characterizations

The phases and crystalline properties are determined by X-ray diffraction (XRD). The surface chemical compositions and electronic structures are checked by X-ray photoelectron spectra (XPS). The morphology and size of particles are analyzed by scanning electron microscopy (SEM) and transmission electron microscopy (TEM). The crystalline microstructures are resolved by the highresolution TEM (HRTEM) and selected area electron diffraction (SAED). The specific surface area, pore volume and size distribution are examined by nitrogen sorption isothermals with Brunauer-Emmett-Teller (BET) and Barrett-Joyner-Halenda (BJH) methods.

Electrochemical measurements

The electrodes are prepared by the following two steps: firstly, a well-dispersed mixture of 70 wt% active materials (as-synthesized KCF) or commercial AC or 918 , 20 wt% acetylene black (AB) conductive agent and 10 wt% polyvinylidene fluoride binder (PVDF, which is dissolved in into the N-methyl-2-pyrrolidone (NMP)) are casted onto the current collectors (Cu foil and carbon-coated Al foil are used for the collectors of anode and cathode respectively.), and followed by drying in a vacuum oven at 110 ^{o}C for 12 h; secondly, the electrodes are pounched into disks with diameter of 12 mm, and the mass loading of active materials was about 1.2~2.5 mg cm^{-2}. The electrochemical performances are examined via CHI660E electrochemical working stations and Neware-CT-4008 testers. Tests for electrodes (KCF, AC, 918) are conducted in half-cells by using the type 2032 coin cells. Tests for LIC (KCF//AC) and Li-DIB (KCF//918) are conducted via full-cells with type 2032 coin cells, with certain mass ratios of anode and cathode active materials. (More detailed information can be seen in **Table S2-3**.) The electrolytes used for KCF and AC electrodes, LIC are 1 M $LiPF_6$ dissolved in the mixed solvents of ethylene carbonate (EC), ethylmethyl carbonate (EMC) and dimethyl carbonate (DMC) (1:1:1 in volume) with 1% vinylene carbonate (VC) additives (LBC-305-01, CAPCHEM, marked A electrolytes). The electrolytes used for KCF and 918 electrodes, Li-DIB are 1 M $LiPF_6$ dissolving in the mixed solvents of ethylene carbonate (EC), ethyl methyl carbonate (EMC) and diethyl carbonate (DEC) (1:1:1 in volume) with the main fluoroethylene carbonate (FEC) additives (LBC-3045I, CAPCHEM, marked B electrolytes). All cell assemblies are performed in a high pure Arfilled dry glovebox (MIKROUNA, O_2 and H_2O<0.1 ppm) and all tests are carried

out at room temperature (about 25 ^{o}C). (The more detailed information of the above-mentioned chemicals, agents and materials can be seen the **Table S1**; the calculations for the m_+/m_-, *C*m, *E*m and *P*m can be seen in the Methods.)

Methods: calculations for C_m, E_m, P_m

The specific capacity (C_m, mAh g^{-1}), energy density ($E_{m,1}$, Wh kg^{-1}) for LIC, energy density ($E_{m,2}$, Wh kg^{-1}) for Li-DIB, and power density (P_m, kW kg^{-1}) are calculated according to the equations **S(1)-S(4)**.

$$C_m = Q_m / 3.6 \quad \textbf{S(1)}$$

$$E_{m,1}\ \textbf{(Capacitor)} = 0.5\ (C_m \triangle V) \quad \textbf{S(2)}$$

$$E_{m,2}\ \textbf{(Battery)} = (C_m V) \quad \textbf{S(3)}$$

$$P_m = 3.6\ E_m / t\textbf{d} \quad \textbf{S(4)}$$

Where m, Q_m, $\triangle V$, V, and *t*d refer to the mass of active materials (mg, for half cells, it means the mass of active materials of anode or cathode; for LIC and Li-DIB full-cells, it means the total masses of active materials of anode and cathode), specific charge or discharge capacity (C g^{-1}, for anode, it means the charge capacity; for cathode and full-cells, it refers to the discharge part), potential window (V), potential of the discharging plateaus (V), and discharging time (s), respectively.

Supplemental figures

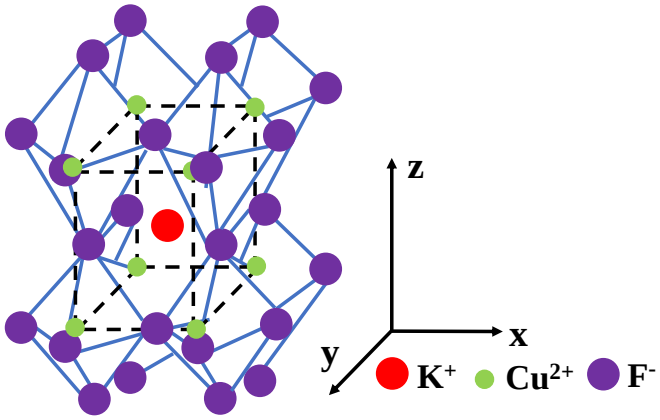

Fig S1. The crystalline structure of KCF sample.

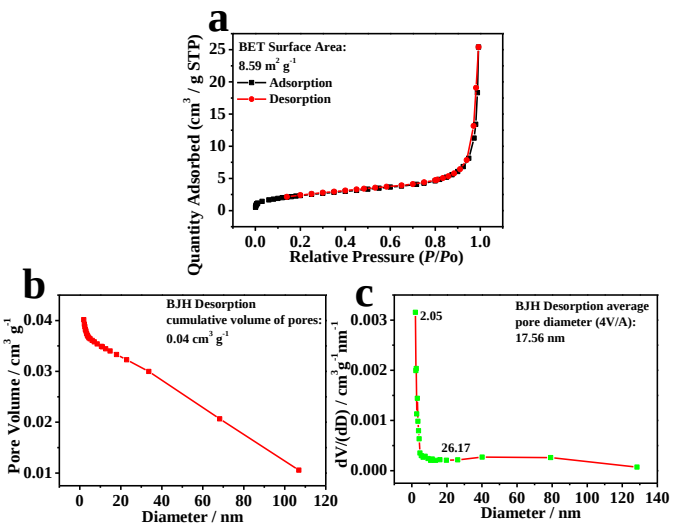

Fig S2. Nitrogen sorption isotherms (a), pore volumes (b) and pore size distributions (c) of KCF sample.

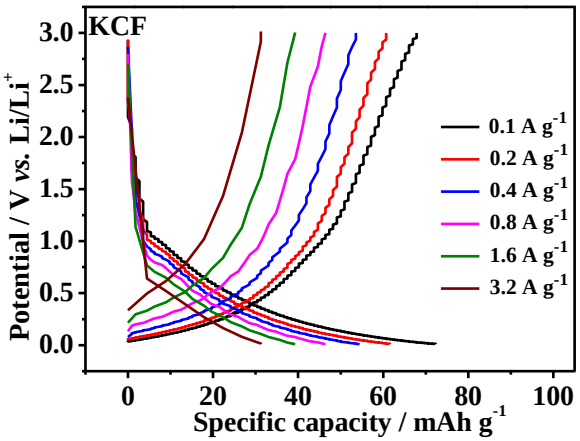

Fig S3. GCD curves for the respective 5th cycle at 0.1-3.2 A g^{-1} of KCF electrode with A electrolytes.

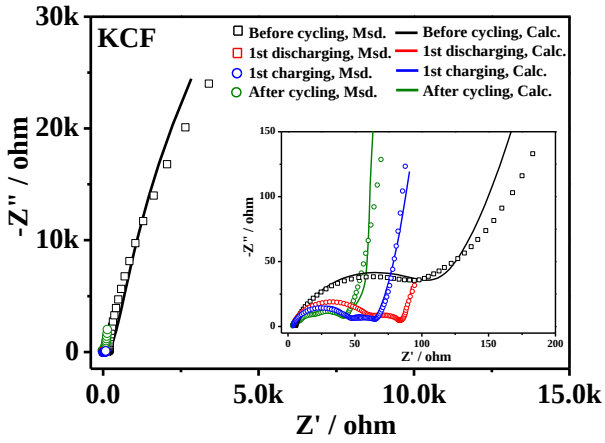

Fig S4. Nyquist plots (the insert is the enlarged high frequency region) of KCF electrode.

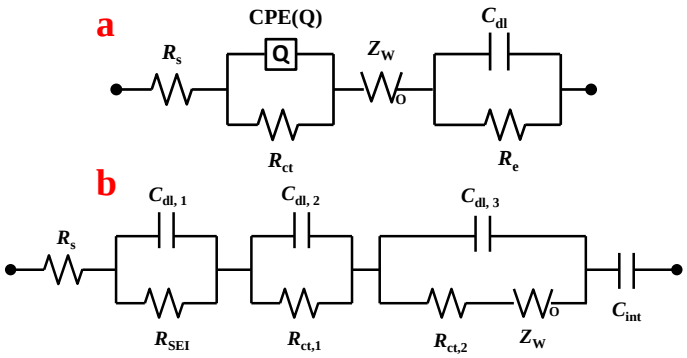

Fig. S5 The equivalent circuits used to fit the experimental Nyquist plots before (a) and after (b) cycling of KCF electrode.

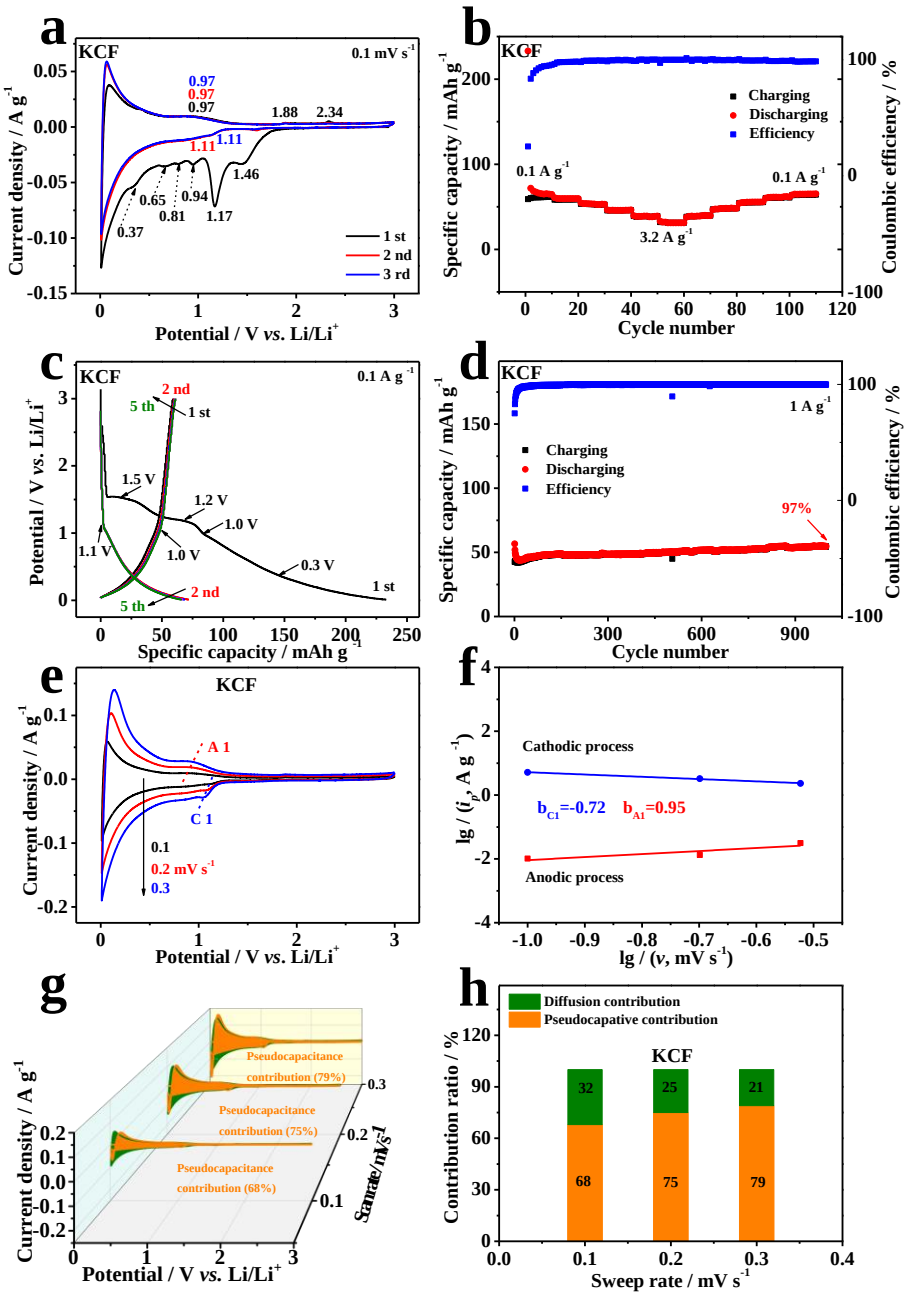

Fig S6. CV plots for the first three cycles at 0.1 mV s^{-1} (a), rate performance and coulombic efficiency at 0.1~3.2~0.1 A g^{-1} (b), GCD curves for the first to fifth cycles at 0.1 A g^{-1} (c), cycling stability for 1000 cycles at 1 A g^{-1} (d), CV plots for the respective third cycle at 0.1, 0.2, 0.3 mV s^{-1} (e), the corresponding relationship of lg*i* *vs*. lg*v* (f), pseudocapacitive contribution (orange region) to the total current contribution at 0.1-0.3 mV s^{-1} (g) and the normalized contribution ratio values of diffusion and pseudocapacitance controlled fractions at 0.1-0.3 mV s^{-1} (h) of the KCF electrode with B electrolytes.

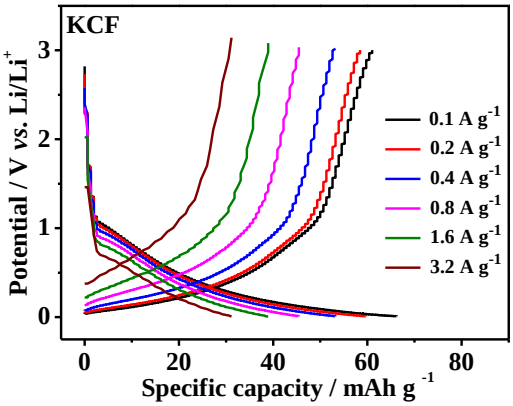

Fig S7. GCD curves for the respective 5th cycle at 0.1-3.2 A g^{-1} of KCF electrode with B electrolytes.

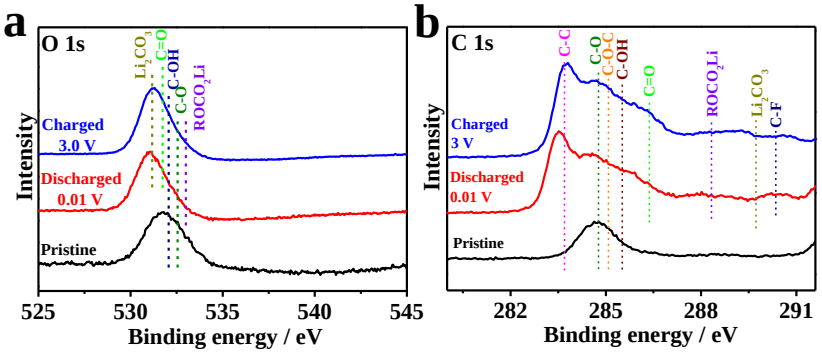

Fig S8. Ex-situ XPS spectra of KCF electrode in pristine, discharged-0.01 V/charged-3.0 V states: O1s-fitted (a) and C1s-fitted (b).

Sample	ICCD-PDF	Crystal system	Space group	Cell (a x b x c) / Å^3
$KCuF_3$	18-1005	Tetragonal	P4mm (99)	4.1429×4.1429×3.926
Cu	04-0836	Cubic	Fm-3m (225)	3.615×3.615×3.615
CuF_2	42-1244	Monoclinic	P21/n (14)	3.2973×4.5624×4.6157
LiF	45-1460	Cubic	Fm-3m	4.027×4.027×4.027
KF	36-1458	Cubic	Fm-3m	5.348×5.348×5.348
Li_2CO_3	22-1141	Monoclinic	C2/c	8.359×4.977×6.194

Fig S9. Crystalline structure information of $KCuF_3$, Cu, CuF_2, LiF and Li_2CO_3 phases.

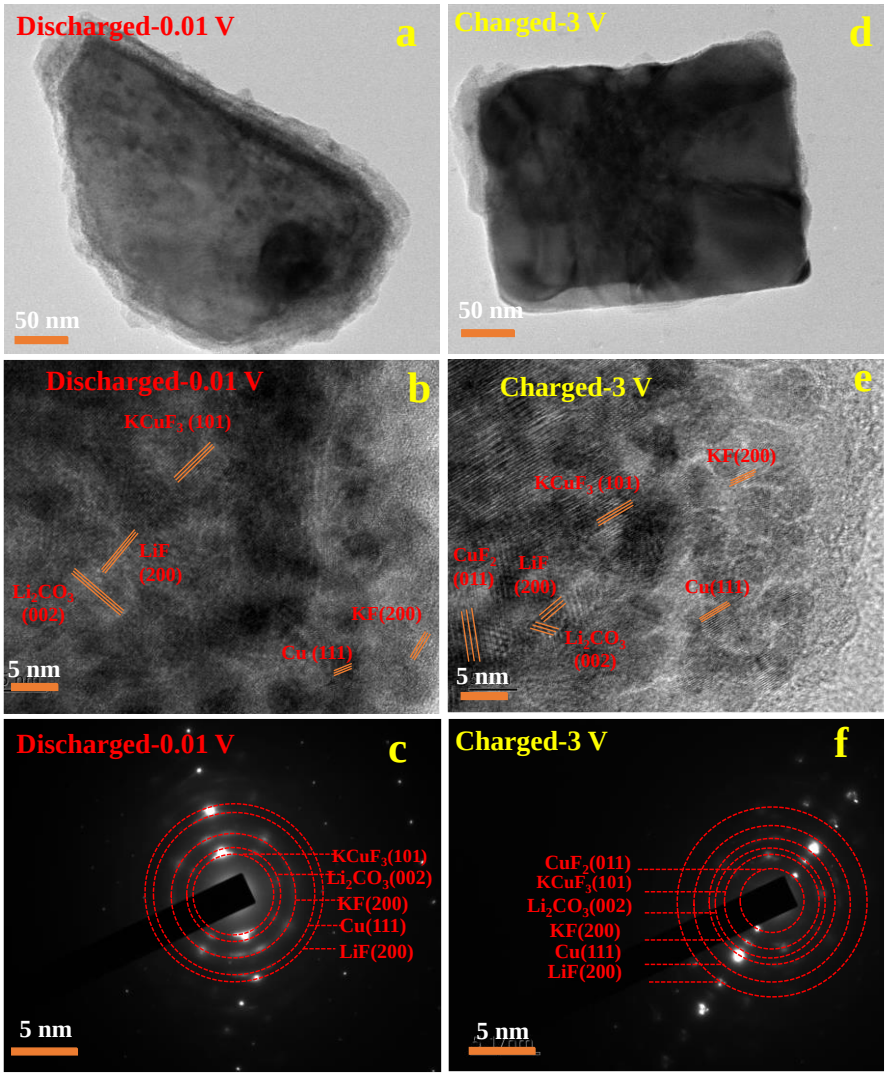

Fig S10. The ex-situ TEM, HRTEM and SEAD pattern of KCF sample in the 1st discharge/charge (0.1 A g^{-1}) state with A electrolytes.

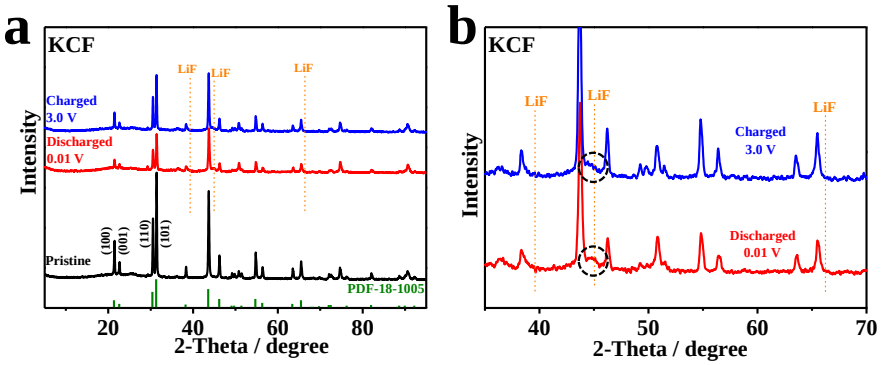

Fig S11. Ex-XRD patterns of KCF electrode in pristine, the 1st discharge/charge (0.1 A g^{-1}) processes with A electrolytes (a); the enlarged region (b).

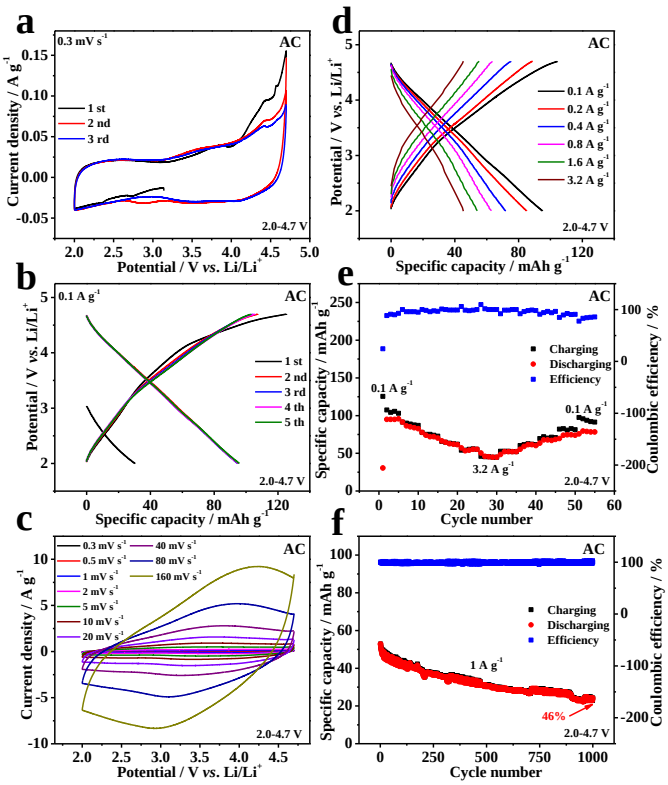

Fig S12. CV plots for the first three cycles at 0.3 mV s^{-1} (a), GCD curves for the first five cycles at 0.1 A g^{-1} (b), CV plots for the respective 3rd cycle at 0.3-160 mV s^{-1} (c), GCD curves for the respective 3rd at 0.1~3.2 A g^{-1} (d), rate performance and coulombic efficiency at 0.1~3.2~0.1 A g^{-1} (e) and cycling stability and coulombic efficiency at 1 A g^{-1} for 1000 cycles (f) of AC electrode with A electrolytes.

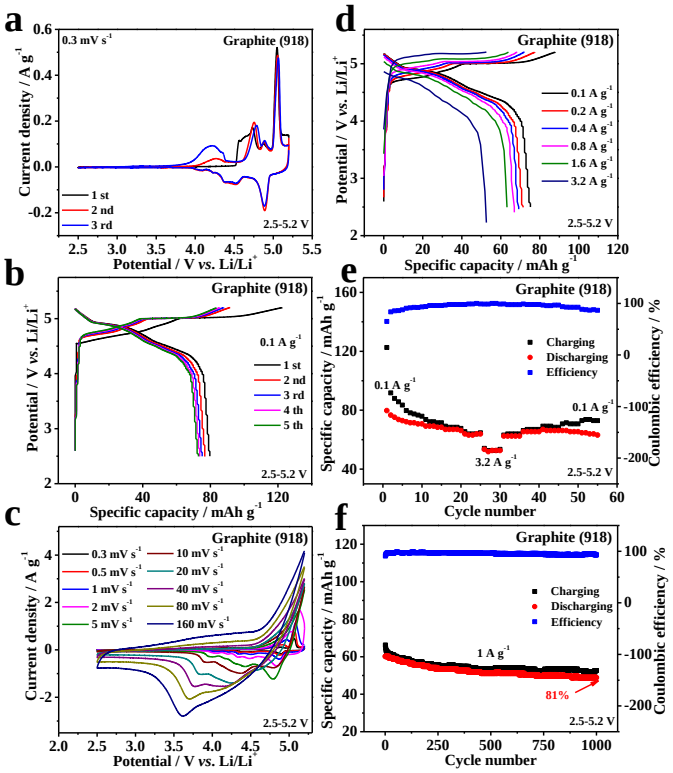

Fig S13. CV plots for the first three cycles at 0.3 mV s^{-1} (a), GCD curves for the first five cycles at 0.1 A g^{-1} (b), CV plots for the respective 3rd cycle at 0.3-160 mV s^{-1} (c), GCD curves for the respective 3rd at 0.1~3.2 A g^{-1} (d), rate performance and coulombic efficiency at 0.1~3.2~0.1 A g^{-1} (e) and cycling stability and coulombic efficiency at 1 A g^{-1} for 1000 cycles (f) of graphite (918) electrode with B electrolytes.

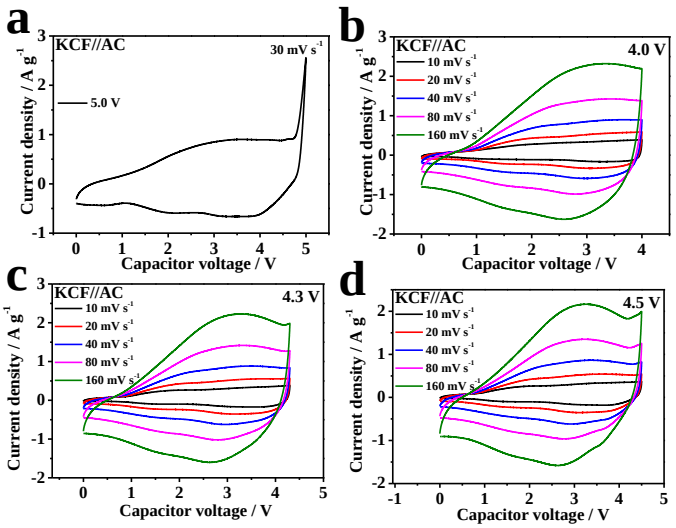

Fig S14. CV windows of KCF//AC LIC with A electrolytes: CV windows at 30 mV s^{-1} under the working voltage of 0-5 V (a), CV plots at 10~160 mV s^{-1} in 4.0 V (b), 4.3 V(c), 4.5 V (d).

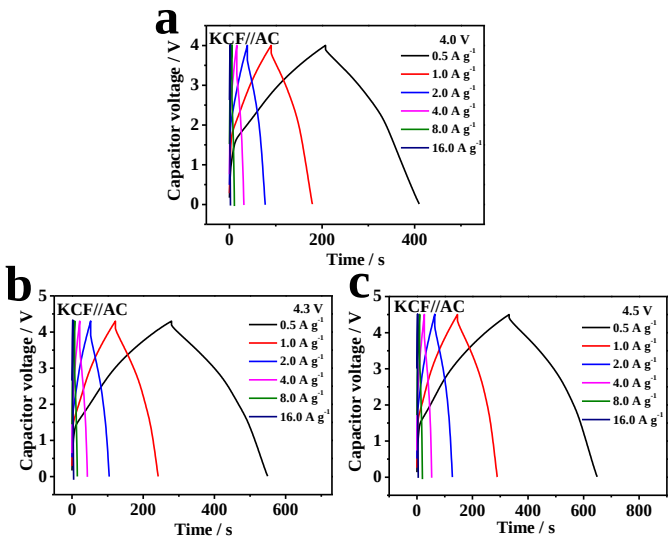

Fig S15. GCD curves of KCF//AC LIC with A electrolytes at 0.5-16.0 A g^{-1} in 4.0 V (a), 4.3 V (b), 4.5 V (c).

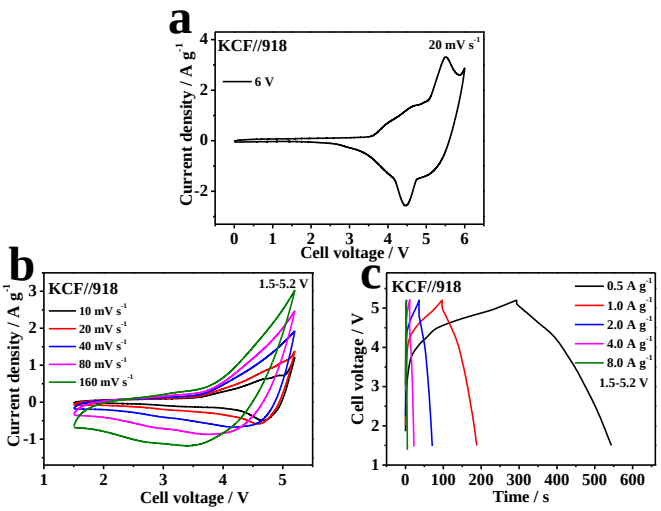

Fig S16. KCF//918 Li-DIB with B electrolytes: CV window at 20 mV s^{-1} under the working voltage of 0-6.0 V (a); CV plots at 10-160 mV s^{-1} (b), GCD curves at 0.5-8.0 A g^{-1} (c) in 1.5-5.2 V.

Supplemental tables

Table S1. Materials, chemicals and reagents used in this study.

Chemials, Agents and Materials	Type	Company	Characteristics
$CuCl_2$•$2H_2O$	AR	SinoPharm	purity≥99.0%
KF•$2H_2O$	AR	SinoPharm	purity≥99.0%
EG	AR	SinoPharm	purity≥99.0%
AC	YEC 8b	FuZhou YiHuan	D50: ~10 μm; Density:> 0.4 g cm^{-3}; SSA:2000~2500 m^2 g^{-1}
Graphite	918	BTR	D50: 17-20 μm; Tab: 0.95-1.2 g cm^{-3}; SSA: 3.0-4.0 m^2 g^{-1}
acetylene black	Battery grade	#	#
NMP	AR	Kermel	purity≥99.0%
PVDF	Battery grade	#	#
A electrolytes	LBC-305-01	CAPCHEM	1 M $LiPF_6$/EC:EMC:DMC (1:1:1) /1% VC
B electrolytes	LBC-3045I	CAPCHEM	1 M $LiPF_6$/EC: EMC: DEC (1:1:1)/FEC, etc.
Li plate	15.6*0.45 mm	China Energy	15.6*0.45 mm
Cu foil	200*0.015	GuangZhou JiaYuan	Total thickness: 15 μm; weight: 87 g m^{-2}
Carbon coated-Al foil	222*0.015	GuagZhou NaNuo	Total thickness: 17 μm; Strength: 192 Mpa
Glass microfiber filters	GF/D 2.7 μm; 1823-025	Whatman	Diameter: 25 mm; Thickness: 675 μm; weight: 121 g m^{-2}
Cell components	CR-2032	ShenZhen TianChenHe	#

Table S2. Specific capacity and cycling stability of anode and cathode and m_+/m_- ratio for KCF//AC LIC and KCF//918 Li-DIB.

Specific capacity of electrodes / (mAh g^{-1})				
Current density / (A g^{-1})	**Anode KCF (0.01-3.0V) with A electrolytes**	**Anode KCF (0.01-3.0 V) with B electrolytes**	**Cathode AC (2.0-4.7 V) with A electrolytes**	**Cathode Graphite (2.5-5.2 V) with B electrolytes**
0.1	65.6	61.1	95.0	75.1
0.2	62.8	58.4	85.1	71.2
0.4	56.1	53.0	72.1	69.0
0.8	55.6	45.8	62.7	66.8
1.6	48.4	39.1	54.0	63.1
3.2	48.1	31.1	45.3	52.5
Cycling behavior Retention% / 1 A g^{-1} / 1000 cycles	191%	97%	46%	81%
m+/m- ratio for KCF//AC LIC based on the Q_m of anode and cathode at 0.1 A g^{-1} with A electrolytes	**1:1.5**			
m+/m- ratio for KCF//918 Li-DIB based on the Q_m of anode and cathode at 0.1 A g^{-1} with B electrolytes	**1:1.2**			

Table S3. EIS parameters of KCF electrode before (a); 1st diacharging/charging and after cycling (b).

a

EIS parameters (Before cycling)	
Model	R(QR)W(CR)
R_s (Ω)	4.834
Q ($S \cdot sec^n$)	1.885×10^{-5}
n	0.8112
R_{ct} (Ω)	93.62
W ($S \cdot sec^{0.5}$)	0.002383
C_{dl} (F)	6.809×10^{-4}
R_e (Ω)	3.513×10^{5}
x^2	3.69×10^{-3}

b

EIS parameters			
KCF	1st diacharging	1st charging	After cycling
Model		R(CR)(CR)(C(RW))C	
R_s (Ω)	4.966	4.866	4.055
$C_{dl,\,1}$ (F)	1.604×10^{-6}	7.954×10^{-6}	1.65×10^{-5}
R_{SEI} (Ω)	39.71	26.49	12.29
$C_{dl,\,2}$ (F)	6.896×10^{-5}	1.984×10^{-6}	3.028×10^{-6}
$R_{ct,\,1}$ (Ω)	36.08	14.12	5.417
$C_{dl,\,3}$ (F)	4.772×10^{-8}	6.589×10^{-4}	8.755×10^{-5}
$R_{ct,\,2}$ (Ω)	0.1455	16.21	18.97
W ($S \cdot sec^{0.5}$)	3.632×10^{-11}	0.09549	0.0226
C_{int} (F)	0.4548	0.1779	0.009038
x^2	1.675×10^{-2}	1.765×10^{-3}	1.776×10^{-3}

Table S4. Performance summary of the KCF//AC LIC and KCF//918 Li-DIB in the study.

Type	Capacitor or Cell system	Working voltage / V	Energy density / Wh kg^{-1}	Power density / kW kg^{-1}	Cycling behavior / retention%, repeated cycles, current density
LIC	KCF//AC with A electrolytes	0.01-4.0	38.4-34.3 28.6-20.6 11.2-7.0	0.7-1.4 2.7-5.0 8.6-19.3	100%/1000/4 A g^{-1} 100%/2000/4 A g^{-1} 100%/3000/4 A g^{-1} 93%/4000/4 A g^{-1} 89%/5000/4 A g^{-1}
		0.01-4.3	55.7-49.2 40.6-29.9 20.5-13.7	0.7-1.5 2.8-5.0 10.0-19.7	91%/1000/4 A g^{-1} 84%/2000/4 A g^{-1} 78%/3000/4 A g^{-1} 71%/4000/4 A g^{-1} 62%/5000/4 A g^{-1}
		0.01-4.5	70.0-63.6 54.7-41.8 28.3-14.2	0.8-1.6 3.1-5.7 10.4-22.2	85%/1000/4 A g^{-1} 63%/2000/4 A g^{-1} 60%/3000/4 A g^{-1} 50%/4000/4 A g^{-1} 48%/5000/4 A g^{-1}
Li-DIB	KCF//918 with B electrolytes	1.5-5.2	70.5-51.5 38.1-22.3-6.4	1.0-2.0 3.9-7.1-9.2	90%/200/4 A g^{-1} 84%/300/4 A g^{-1} 78%/500/4 A g^{-1} 72%/1000/4 A g^{-1} 65%/2000/4 A g^{-1} 48%/5000/4 A g^{-1}

Table S5. A comparison for the performance of the KCF//AC LIC in the study with some reported LICs in literature.

LICs	Working voltage / V	Energy density / Wh kg^{-1}	Power density / kW kg^{-1}	Cycling behavior / retention%, repeated cycles, current density	Refs.
$LiNi_{0.5}Mn_{1.5}O_4$//AC	1.5-3.25	19-8	0.13-3.5	81%/3000/1 A g^{-1}	1
TiO_2 -B//CNT	0.0-2.8	23-7	0.14-2.8	73%/1200/1.5 A g^{-1}	2
F−Fe_2O_3//AC	0-3	28	2.5	90%/5000/2.25 A g^{-1}	3
H-TiO_2/PPy/SWCNTs//AC	1.0-3.0	31.3-1.9	0.2-4.0	77.8%/3000/0.5 A g^{-1}	4
TiO_2/graphene//AC	1.0-3.0	42-8.9	0.8-8	100%/6500/4 A g^{-1}	5
T-Nb_2O_5/Graphene paper//AC	0.5-3.0	47-15	0.39-18	93%/2000/0.25 A g^{-1}	6
TiS_2//AC	0−2.6	49	0.1	76%/2000/1 A g^{-1}	7
NBC//$LiMn_2O_4$	0-2.3	50-17	0.57-6.9	88%/5000/3 A g^{-1}	8
FeS_2/C//AC	0-3.2	63-5	0.15-4	100%/2500/2 A g^{-1}	9
AC/TiO_2@PCNF-12	0.0-3.0	67.4-27.5	0.075-5	85%/10000/10 A g^{-1}	10
KCF//AC	0.01-4.0	38.4-34.3 28.6-20.6 11.2-7.0	0.7-1.4 2.7-5.0 8.6-19.3	100%/1000/4 A g^{-1} 100%/2000/4 A g^{-1} 100%/3000/4 A g^{-1} 93%/4000/4 A g^{-1} 89%/5000/4 A g^{-1}	**This work**
	0.01-4.3	55.7-49.2 40.6-29.9 20.5-13.7	0.7-1.5 2.8-5.0 10.0-19.7	91%/1000/4 A g^{-1} 84%/2000/4 A g^{-1} 78%/3000/4 A g^{-1} 71%/4000/4 A g^{-1} 62%/5000/4 A g^{-1}	
	0.01-4.5	70.0-63.6 54.7-41.8 28.3-14.2	0.8-1.6 3.1-5.7 10.4-22.2	85%/1000/4 A g^{-1} 63%/2000/4 A g^{-1} 60%/3000/4 A g^{-1} 50%/4000/4 A g^{-1} 48%/5000/4 A g^{-1}	

Table S6. A comparison for the performance of the KCF//918 Li-DIB in the study with some reported Li/Na-DIBs in literature.

Li/Na-DIBs	**Working voltage / V**	**Energy density / Wh kg^{-1}**	**Power density / kW kg^{-1}**	**Cycling behavior / retention%, repeated cycles, current density**	**Refs.**
WS_2//Graphite	0-4	36	#	59%/30/0.1 A g^{-1}	11
TiO_2//Graphite	1.5-3.7	36	#	88%/50/0.1 A g^{-1}	12
Carbon-coated $NaTi_2(PO_4)_3$//$Ni(OH)_2$	0.2-1.4	40.1	0.2577	87%/500/10 C	13
$Ti_3C_2T_x$//Graphite	0-3.2	40	1.608	85%/200/0.33 A g^{-1}	14
Nb_2O_5//Graphite	1.5-3.5	52	#	84%/100/0.1 A g^{-1}	15
Si-compound//Graphite	0-3	54	#	53%/100/0.1 A g^{-1}	16
RGO//Graphite	0-4	70	1.33	74%/50/1.33 A g^{-1}	17
KCF//918	1.5-5.2	70.5-51.5 38.1-23.3-6.4	1.0-2.0 3.9-7.1-9.2	90%/200/4 A g^{-1} 84%/300/4 A g^{-1} 78%/500/4 A g^{-1} 72%/1000/4 A g^{-1} 65%/2000/4 A g^{-1} 48%/5000/4 A g^{-1}	**This work**

References

In Table S5

1 N. Arun, A. Jain, V. Aravindan, S. Jayaraman, W. C. Ling, M. P. Srinivasan, S. Madhavi, *Nano Energy*, 2015, **12**, 69-75.

2 V. Aravindan, N. Shubha, W. C. Ling, S. Madhavi, *J. Mater. Chem. A*, 2013, **1**, 6145-6151.

3 K. Karthikeyan, S. Amaresh, S. N. Lee, V. Aravindan, Y. S. Lee, *Chem. Asian J.*, 2014, **9**, 852-857.

4 G. Tang, L. J. Cao, P. Xiao, Y. H. Zhang, H. Liu, *J. Power Sources*, 2017, **355**, 1-7.

5 H. Kim, M.-Y. Cho, M.-H. Kim, K.-Y. Park, H. Gwon, Y. Lee, K. C. Roh, K. Kang, *Adv. Energy Mater.*, 2013, **3**, 1500-1506.

6 L. P. Kong, C. F. Zhang, J. T. Wang, W. M. Qiao, L. C. Ling, D. H. Long, *ACS Nano*, 2015, **9**, 11200-11208.

7 A. Chaturvedi, P. Hu, V. Aravindan, C. Kloc, S. Madhavi, *J. Mater. Chem. A*, 2017, **5**, 9177-9181.

8 C. Y. Li, W. Z. Wu, S. S. Zhang, L. He, Y. S. Zhu, J. Wang, L. J. Fu, Y. H. Chen, Y. P. Wu and W. Huang, *J. Mater. Chem. A*, 2019, **7**, 4110-4118.

9 D. T. Pham, J. P. Baboo, J. Song, S. Kim, J. Jo, V. Mathew, M. H. Alfaruqi, B. Sambandam and J. Kim, *Nanoscale*, 2018, **10**, 5938-5949.

10 C. Yang, J. L. Lan, W. X. Liu, Y. Liu, Y. H. Yu, X. P. Yang, *ACS Appl. Mater. Interfaces*, 2017, **9**, 18710-18719.

In Table S6

11 S. Bellani, F. Wang, G. Longoni, L. Najafi, R. Oropesa-Nunez, A. E. Del Rio Castillo, M. Prato, X. Zhuang, V. Pellegrini, X. Feng and F. Bonaccorso, *Nano Lett.*, 2018, **18**, 7155-7164.

12 A. K. Thapa, G. Park, H. Nakamura, T. Ishihara, N. Moriyama, T. Kawamura, H. Wang, M. Yoshio, *Electrochim. Acta*, 2010, **55**, 7305-7309.

13 Q. S. Nian, S. Liu, J. Liu, Q. Zhang, J. Q. Shi, C. Liu, R. Wang, Z. L. Tao, J. Chen, *ACS Appl. Energy Mater.,* 2019, **2**, 4370−4378.

14 X. Y. Shi, T. Deng, G. S. Zhu, *Ceram. Int.*, 2020, **46**, 24887-24892.

15 G. Park, N. Gunawardhana, C. Lee, S.-M. Lee, Y.-S. Lee, M. Yoshio, *J. Power Sources*, 2013, **236**, 145-150.

16 H. Nakano, Y. Sugiyama, T. Morishita, M. J. S. Spencer, I. K. Snook, Y. Kumai, H. Okamoto, *J. Mater. Chem. A*, 2014, **2**, 7588-7592.

17 X. Y. Shi, W. Zhang, J. F. Wang, W. T. Zheng, K. K. Huang, H. B. Zhang, S. H. Feng, H. Chen, *Adv. Energy Mater.*, 2016, **6**, 1601378.